THE JOURNAL OF PHYSICAL CHEMISTRY C

Article

pubs.acs.org/JPCC

Photoelectron Spectroscopy and Density Functional Calculations of VGe_n^- (n = 3−12) Clusters

Xiao-Jiao Deng, Xiang-Yu Kong, Hong-Guang Xu,* Xi-Ling Xu, Gang Feng, and Wei-Jun Zheng*

Beijing National Laboratory for Molecular Sciences, State Key Laboratory of Molecular Reaction Dynamics, Institute of Chemistry, Chinese Academy of Sciences, Beijing 100190, China

Supporting Information

ABSTRACT: The structural, electronic and magnetic properties of $VGe_n^{-/0}$ (n = 3−12) clusters were investigated using anion photoelectron spectroscopy in combination with density functional theory calculations. We found that the dominant geometries are exohedral for the $VGe_n^{-/0}$ clusters with $n \leq 7$. The $VGe_8^{-/0}$ clusters have half-encapsulated boat-shaped structures, and the opening of the boat-shaped structure is gradually covered by the additional Ge atoms to form Ge_n cage from n = 9−11. At n = 12, a D_{3d} distorted hexagonal prism cage structure is formed. According to the natural population analysis, for both anionic and neutral VGe_n clusters of n = 8−12, there is electron transfer from the Ge_n framework to the V atom and the total magnetic moments decrease to the minima. The electron transfer pattern and the minimization of the magnetic moments for these clusters are related to their structural evolution.

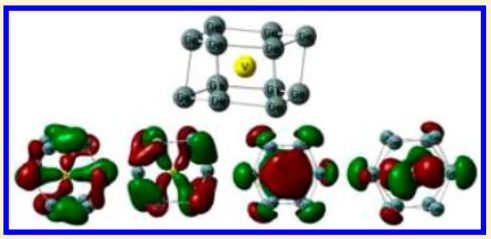

1. INTRODUCTION

Germanium is one of the most important alternatives to silicon in the field of the semiconductor materials because of its superior electron and hole mobilities.[1,2] Although pure germanium clusters are not able to form fullerene-like cage structures, some theoretical and experimental studies suggested that the doping of a transition metal (TM) atom can stabilize Ge cage structures analogous to the case of TM-doped silicon clusters.[3−6] The stable TM-doped germanium clusters may be used as building blocks for cluster-assembled materials and may have potential applications in many fields.[7−25] It has been suggested by calculations that metal-doped germanium clusters display different growth behavior from the metal-doped silicon clusters.[26,27] The mass spectrometric stability investigation on metal-doped Si, Ge, Sn, and Pb clusters showed that the enhanced stabilities are likely related to the formation of cage-like structures and the stability patterns depend on both host and dopant atoms.[28] The theoretical studies of Wang et al.[5,18,29,30] also suggested that the growth pattern and properties of $TMGe_n$ clusters depend on the nature of doped TM impurities, for example, the structural and electronic features of WGe_n are very different from those of Cu, Zn, or Ni-doped Ge_n clusters.

Vanadium is an important metal widely used in alloy industries. In our previous studies, we found that the two V atoms are tightly bonded in V_2Si_n clusters,[31] and the V_2Si_{20} cluster has a V_2 unit encapsulated inside an elongated dodecahedron, thus, forms the smallest fullerene-like silicon cage.[32] Regarding vanadium-doped germanium clusters, there are also a number of studies in the literature. Singh et al. have investigated the stability of germanium nanotubes doped with V atoms using density functional theory (DFT) calculations and suggested the infinite V-doped Ge nanotubes to be metallic.[33] Bandyopadhyay et al. investigated the relative stability of Sc, Ti, and V encapsulating Ge_n clusters in the size range of n = 14−20 using DFT calculations and suggested that the enhanced stability of some clusters can be explained by the formation of a filled shell free-electron gas or geometric effects.[20] Tang et al. studied the geometric, optical, and magnetic properties of $V@Ge_{12}$ and the other 3d-$TM@Ge_{12}$ clusters.[22] Very recently, Atobe et al.[34] investigated a number of TM-doped Ge clusters including VGe_n by mass spectrometry, anion photoelectron spectroscopy, and H_2O adsorption reactivity experiments and suggested that VGe_{16}^+ can be considered as a germanium-based superatom. In this work, in order to get more detailed information about the structural, electronic and magnetic properties of V-doped germanium clusters, we investigated VGe_n^- (n = 3−12) clusters using anion photoelectron spectroscopy combined with DFT calculations.

2. EXPERIMENTAL AND THEORETICAL METHODS

2.1. Experimental Method. The experiments were conducted on a home-built apparatus equipped with a laser vaporization cluster source, a time-of-flight mass spectrometer, and a magnetic-bottle photoelectron spectrometer, which has been described elsewhere.[31] The VGe_n^- clusters were generated in the laser vaporization source by laser ablation of a rotating and translating disk target (13 mm diameter, V/Ge mole ratio 1:2) with the second harmonic of a nanosecond Nd:YAG laser (Continuum Surelite II-10). The typical laser power used in this work was about 10 mJ/pulse. Helium gas with ∼4 atm backing

Special Issue: Current Trends in Clusters and Nanoparticles Conference

Received: November 22, 2014
Revised: December 25, 2014
Published: December 30, 2014

DOI: 10.1021/jp511694c
J. Phys. Chem. C 2015, 119, 11048−11055

pressure was allowed to expand through a pulsed valve (General Valve Series 9) into the source to cool the formed clusters. The generated cluster anions were mass-analyzed with the time-of-flight mass spectrometer. The VGe_n^- (n = 3−12) cluster anions were selected with a mass gate, decelerated by a momentum decelerator, and crossed with the beam of another Nd:YAG laser (Continuum Surelite II-10, 266 nm) at the photodetachment region. The electrons from photodetachment were energy-analyzed by the magnetic-bottle photoelectron spectrometer. The photoelectron spectra were calibrated with the spectra of Cu^- and Pb^- taken at similar conditions. The resolution of the magnetic-bottle photoelectron spectrometer was about 40 meV at electron kinetic energy of 1 eV.

2.2. Theoretical Method. All calculations were conducted with the Gaussian 09 program package.[35] Geometry optimizations of the VGe_n^- (n = 3−12) clusters were performed using DFT with the spin unrestricted Becke three-parameter exchange and the Perdew−Wang generalized gradient approximation functional (B3PW91).[36−39] The 6-311+G(d) basis set was used for the V and Ge atoms. For all clusters, a large amount of initial structures were taken into account at all possible spin states, such as V-capping or V-substituting of pure Ge_n clusters, the reported structures of TM-doped Ge_n or TM-doped Si_n clusters in the literature.[5,12,18,21,29,30,40] All geometries were optimized without any symmetry constraint. Harmonic vibrational frequencies were calculated to make sure that the structures correspond to real local minima, and the zero-point vibrational energy corrections were included for the relative energies of isomers. The natural population analysis (NPA) was conducted using the Nature Bond Orbital (NBO) version 3.1 program[41−48] implemented in the Gaussian 09 package.

3. EXPERIMENTAL RESULTS

The photoelectron spectra of VGe_n^- (n = 3−12) clusters recorded with 266 nm photons are shown in Figure 1. The vertical detachment energies (VDEs) and adiabatic detachment energies (ADEs) of these clusters obtained from the photoelectron spectra are summarized in Table 1. The ADEs of these clusters were determined by drawing a straight line along the leading edge of the first peaks to cross the baseline of spectra and adding the instrumental resolution to the electron binding energy (EBE) values at the crossing points. The VDEs of these clusters were estimated from the maxima of the peaks. In Figure 1, the spectra of VGe_n^- (n = 5−12) clusters measured by us are similar to those reported in ref 34, except that some of the broad peaks in ref 34 are resolved into several sharp peaks in this work because the low energy photons (266 nm) were used.

As shown in Figure 1, the spectrum of VGe_3^- has five major peaks centered at 2.02, 2.80, 3.13, 3.40, and 3.60 eV, respectively. VGe_4^- has four resolved peaks centered at 2.47, 2.84, 3.20, and 3.60 eV and a barely resolved peak at ∼4.09 eV. The spectrum of VGe_5^- shows a small peak at 2.45 eV, followed with three resolved peaks centered at 3.19, 3.37, and 3.56 eV. The spectrum of VGe_6^- has a small peak centered at 2.63 eV, followed with a shoulder at 3.23 eV and three barely resolved peaks at 3.43, 3.77, and 4.16 eV. The spectrum of VGe_7^- shows similar features with that of VGe_6^-, there is a resolved peak centered at 2.96 eV and two broad peaks centered at 3.62 and 3.90 eV. Three discernible peaks centered at 3.33, 3.76, and 3.99 eV can be observed in the spectrum of VGe_8^-. The spectrum of VGe_9^- is similar to that of VGe_8^-, having two peaks centered at 3.42 and 4.07 eV, suggesting that they may have similar structural features. In the spectrum of VGe_{10}^-, three peaks centered at 3.44, 3.69, and 4.26 eV, respectively, can be observed. For VGe_{11}^-, there are two barely resolved peaks, with one of them centered at ∼4.0 eV and the other located above 4.2 eV. Besides, there is a shoulder at ∼3.85 eV. The spectrum of VGe_{12}^- has an unresolved peak in the range of 3.5−4.4 eV, and the VDE can be tentatively assigned as 3.7 eV.

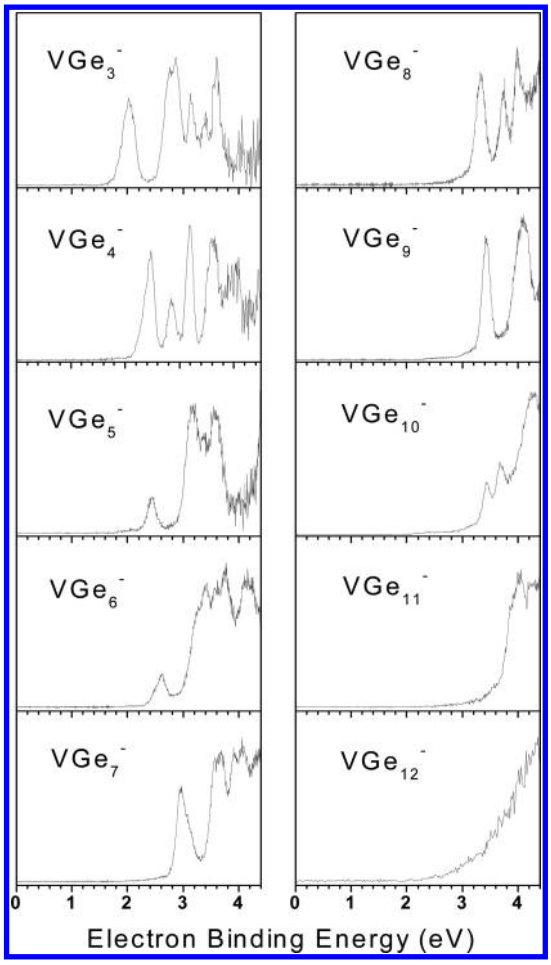

Figure 1. Photoelectron spectra of VGe_n^- (n = 3−12) clusters recorded with 266 nm photons.

Table 1. Experimentally Observed VDEs and ADEs from the Photoelectron Spectra of VGe_n^- (n = 3−12)[a]

cluster	ADE (eV)	VDEs of the peaks (eV)
VGe_3^-	1.73	2.20, 2.80, 3.13, 3.40, 3.60
VGe_4^-	2.20	2.47, 2.84, 3.20, 3.60, 4.09
VGe_5^-	2.26	2.45, 3.19, 3.37, 3.56
VGe_6^-	2.33	2.63, 3.43, 3.77, 4.16
VGe_7^-	2.78	2.96, 3.62, 3.90
VGe_8^-	3.14	3.33, 3.76, 3.99
VGe_9^-	3.26	3.42, 4.07,
VGe_{10}^-	3.26	3.44, 3.69, 4.26
VGe_{11}^-	3.6 ± 0.2	3.85 ± 0.2, 4.0 ± 0.2, 4.2 ± 0.2
VGe_{12}^-	3.4 ± 0.2	3.7 ± 0.2

[a]The uncertainties of the ADE and VDE values are ±0.08 eV, unless specified.

4. THEORETICAL RESULTS

We have optimized the structures of VGe_n^- (n = 3−12) clusters with B3PW91 functional, and the typical low-lying isomers are presented in Figure 2 with the most stable ones on the left.

DOI: 10.1021/jp511694c
J. Phys. Chem. C 2015, 119, 11048−11055

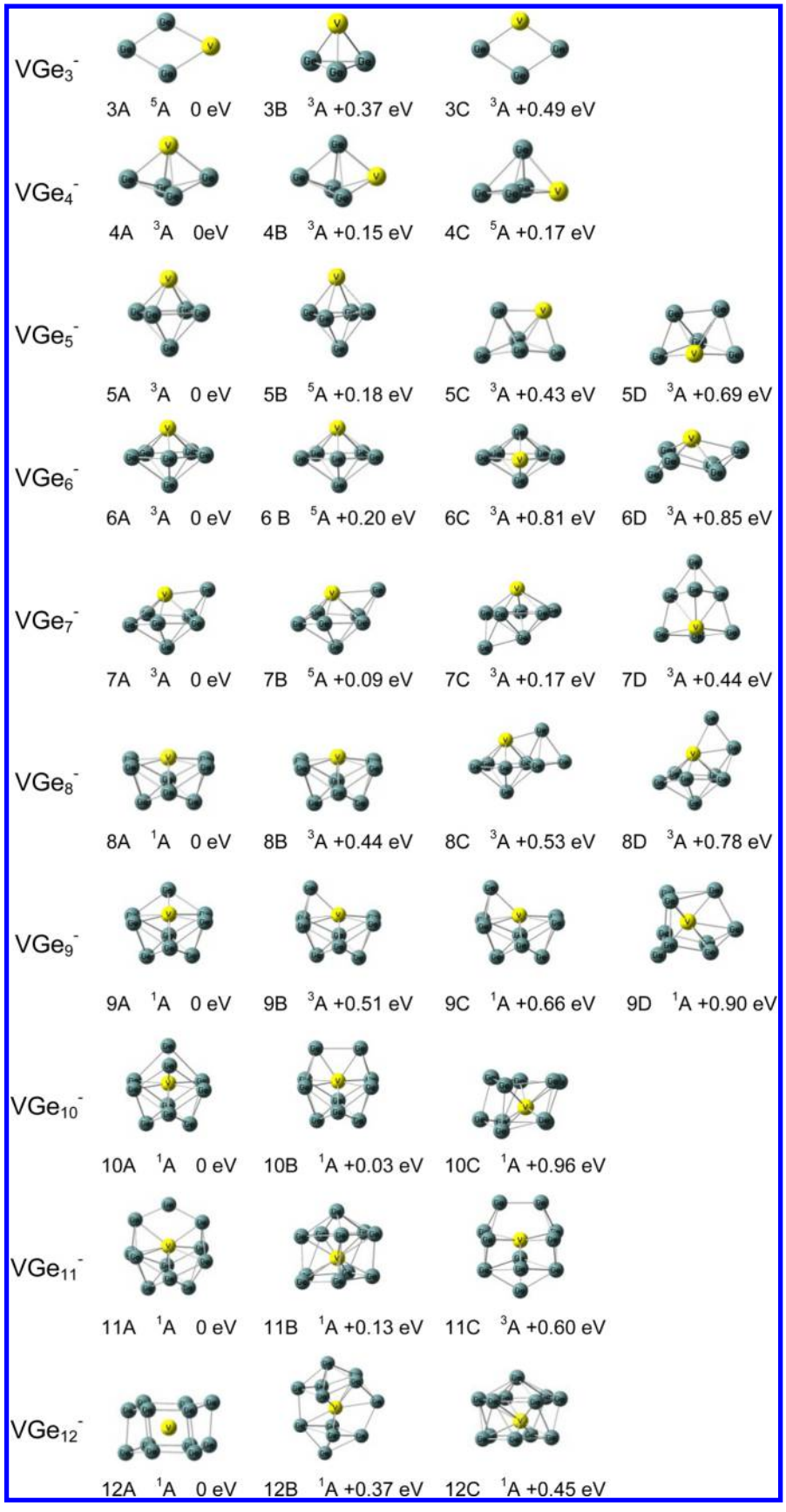

Figure 2. Geometries of the typical low-lying isomers of VGe_n^- (n = 3−12) clusters. The relative energies to the most stable isomers are shown.

The relative energies of these isomers as well as their theoretical VDEs and ADEs are summarized in Table 2. The Cartesian coordinates of the low-lying isomers of VGe_n^- (n = 3−12) are available in the Supporting Information.

DOI: 10.1021/jp511694c
J. Phys. Chem. C 2015, 119, 11048−11055

Table 2. Relative Energies of the Low Energy Isomers of the VGe_n^- (n = 3−12) as Well as Their VDEs and ADEs Obtained by DFT Calculations

isomer					VDE (eV)		ADE (eV)	
		sym.	state	ΔE (eV)	theo.	expt.	theo.	expt.
VGe_3^-	**3A**	C_{2v}	^{5}A	0	1.94	2.02	1.93	1.73
	3B	C_s	^{3}A	0.37	1.73		1.56	
	3C	C_s	^{3}A	0.49	1.93		1.57	
VGe_4^-	**4A**	C_{2v}	^{3}A	0	2.44	2.47	2.09	2.20
	4B	C_s	^{3}A	0.15	2.33		2.01	
	4C	C_s	^{5}A	0.17	2.14		1.88	
VGe_5^-	**5A**	C_{4v}	^{3}A	0	2.76	2.45	2.32	2.26
	5B	C_{2v}	^{5}A	0.18	2.23		2.15	
	5C	C_s	^{3}A	0.43	2.21		1.88	
	5D	C_1	^{3}A	0.69	2.36		1.62	
VGe_6^-	**6A**	C_{5v}	^{3}A	0	2.96	2.63	2.79	2.33
	6B	C_1	^{5}A	0.20	2.75		2.73	
	6C	C_{2v}	^{5}A	0.64	2.06		2.05	
	6D	C_s	^{3}A	0.81	2.46		2.20	
VGe_7^-	**7A**	C_s	^{3}A	0	2.72	2.96	2.48	2.78
	7B	C_s	^{5}A	0.09	2.47		2.39	
	7C	C_s	^{3}A	0.17	2.38		2.29	
	7D	C_s	^{3}A	0.44	2.69		2.51	
VGe_8^-	**8A**	C_{2v}	^{1}A	0	3.22	3.33	3.08	3.14
	8B	C_{2v}	^{3}A	0.44	2.67		2.64	
	8C	C_s	^{3}A	0.53	2.94		2.85	
	8D	C_s	^{3}A	0.78	3.13		2.29	
VGe_9^-	**9A**	C_{3v}	^{1}A	0	3.35	3.42	3.26	3.26
	9B	C_s	^{3}A	0.51	3.24		3.11	
	9C	C_s	^{1}A	0.66	3.10		2.96	
	9D	C_{3v}	^{1}A	0.90	3.65		3.58	
VGe_{10}^-	**10A**	C_1	^{1}A	0	3.56	3.44	3.26	3.26
	10B	C_s	^{1}A	0.03	3.79		3.56	
	10C	C_1	^{1}A	0.96	3.38		3.24	
VGe_{11}^-	**11A**	C_1	^{1}A	0	3.71	3.85	3.59	3.6
	11B	C_1	^{1}A	0.13	3.52		3.12	
	11C	C_1	^{3}A	0.60	3.23		2.96	
VGe_{12}^-	**12A**	D_{3d}	^{1}A	0	3.63	3.7	3.51	3.4
	12B	C_s	^{1}A	0.37	3.64		3.44	
	12C	C_s	^{1}A	0.45	3.46		3.40	

4.1. Anionic VGe_n^- (n = 3−12) Clusters. *VGe_3^-*. The most stable structure of VGe_3^- (isomer **3A**) is a rhombus with C_{2v} symmetry, and its theoretical VDE is 1.94 eV, close to the experimental value (2.02 eV). Isomer **3B** is a tetrahedron, and its energy is 0.37 eV higher than **3A**. Isomer **3C** is also a rhombus, and it is 0.49 eV higher than **3A** in energy. Therefore, we suggest that isomer **3A** is the most likely isomer observed in our experiments.

VGe_4^-. For VGe_4^- cluster, isomers **4A** and **4B** are triangular bipyramids with the V atom at different location. Isomer **4A** can also be considered as the V atom interacting with a bent Ge_4 rhombus, while isomer **4B** can be viewed as the V atom capping a Ge_4 tetrahedron. Isomer **4B** is higher in energy than **4A** by 0.15 eV. The VDEs of isomers **4A** and **4B** are calculated to be 2.44 and 2.33 eV respectively, both are very close to the experimental value (2.47 eV). Isomer **4C** is a distorted square pyramid with the V atom at the square base. The energy of **4C** is higher than **4A** by 0.17 eV, and its theoretical VDE (2.14 eV) deviates from the experimental value. Therefore, we suggest that isomer **4A** is the most likely structure detected in our experiments, but the existence of **4B** cannot be ruled out.

VGe_5^-. The first two isomers of VGe_5^- cluster (**5A** and **5B**) are square bipyramids, and **5B** is higher than **5A** by 0.18 eV in energy. Isomers **5C** and **5D** can be viewed as a Ge atom capping on the different faces of VGe_4 triangle bipyramid. Isomers **5C** and **5D** can be ruled out because they are less stable than **5A** by 0.43 and 0.69 eV in energy, respectively. The calculated VDE of isomer **5A** is 2.76 eV, which is slightly overestimated compared with the experimental value of 2.45 eV, but can still be regarded as a reasonable agreement at this level of theory. The theoretical VDE of **5B** (2.23 eV) is also in reasonable agreement with the first peak in the spectrum of VGe_5^- (2.45 eV). Therefore, we suggest that isomers **5A** and **5B** coexist in our experiments.

VGe_6^-. The most stable isomer of VGe_6^- (**6A**) is a pentagonal bipyramid with the V atom at the vertex. The structure of isomer **6B** is similar to that of **6A** but with different spin multiplicity, and it is higher in energy than **6A** by 0.20 eV. Isomer **6B** can be considered as a low-lying electronic excited state of isomer **6A**. Isomer **6C** is also a pentagonal bipyramid but with the V atom at the equatorial ring. Isomer **6D** can be viewed as the V atom locating above a chair-shaped Ge_6 ring. The calculated VDE of **6A** is 2.96 eV, and it may be considered as contributing to the shoulder at 3.23 eV in the experimental spectrum. The theoretical VDE of **6B** is calculated to be 2.75 eV, in good agreement with the VDE of the first peak in the experimental spectrum (2.63 eV). Thus, isomers **6A** and **6B** are suggested to be the probable ones detected in our experiments. The existence of isomers **6C** and **6D** in the cluster beam can be ruled out because they are much less stable than isomer **6A**.

VGe_7^-. For VGe_7^- cluster, isomers **7A** and **7B** can be seen as a Ge atom capping one of the upper faces of the distorted VGe_6 pentagonal bipyramid, but with different spin multiplicities. Isomer **7C** can be considered as a Ge atom capping one of the lower faces of the distorted VGe_6 pentagonal bipyramid. The calculated VDE of **7A** (2.72 eV) agrees with the experimental value (2.96 eV), but those of **7B** and **7C** (2.47 and 2.38 eV) are much lower than the experimental measurement. Isomer **7D** is 0.44 eV higher than **7A** in energy. Thus, we suggest isomer **7A** to be the most likely structure observed in our experiments. This is consistent with the similar spectral features of VGe_6^- and VGe_7^- observed in experiments.

VGe_8^-. The most stable isomer of VGe_8^- (**8A**) can be viewed as a half-endohedral structure with the V atom locating in a boat-shaped Ge_8 framework. Isomer **8A** also can be seen as two square bipyramids sharing one face. Isomer **8B** has a structure similar to that of **8A** but with different multiplicity, and it is higher in energy than **8A** by 0.44 eV. Isomer **8C** can be considered as two Ge atoms capping on a VGe_6 pentagonal bipyramid. Isomer **8D** can be obtained by bonding three Ge atoms to the VGe_5 tetragonal bipyramid. The calculated VDE of **8A** (3.22 eV) is in good agreement with the experimental value (3.33 eV). The calculated VDEs of **8B** and **8C** deviate from the experimental result, and they are less stable than **8A** in energy. The energy of isomer **8D** is higher than **8A** by 0.78 eV. Therefore, the existence of isomers **8B**, **8C**, and **8D** can be ruled out. We suggest isomer **8A** to be the most probable isomer contributing to the experimental spectrum.

VGe_9^-. For VGe_9^-, isomers **9A**, **9B**, and **9C** can be viewed as a Ge atom capping the different location of boat-shaped structure of VGe_8^- (**8A**). Isomers **9B** and **9C** have similar structures with different spin multiplicities, and they are 0.51 and 0.66 eV higher

DOI: 10.1021/jp511694c
J. Phys. Chem. C 2015, 119, 11048−11055

than **9A** in energy, respectively. Isomer **9D** can be described as three Ge atoms capping the chair-shaped structure of VGe_6^- (**6C**), and its energy is 0.90 eV higher than **9A**. The calculated VDE of **9A** (3.35 eV) is in agreement with the experimental value (3.42 eV), thus, it is considered as the most probable one detected in our experiments. This is also in agreement with the experimental result that VGe_8^- and VGe_9^- have similar spectral features. The existence of isomers **9B**, **9C**, and **9D** can be excluded because they are much less stable than **9A**.

VGe_{10}^-. With respect to VGe_{10}^-, all of the low-lying isomers are endohedral structures. Isomers **10A** and **10B** can be regarded as two Ge atoms connecting to different locations of the boat-shaped structure of VGe_8^- (**8A**). Isomer **10B** is higher in energy than **10A** by only 0.03 eV. The calculated VDE of isomer **10A** is 3.56 eV, in reasonable agreement with the experimental measurement (3.44 eV). Although the calculated VDE of **10B** (3.79 eV) is higher than the first peak of the experimental spectrum, it can be considered as contributing to the features of higher binding energy in the experimental spectrum. The structure of isomer **10C** is an oblique pentagonal prism with the V atom at the center. Its presence in the experiment is unlikely because it is much less stable than **10A** by 0.96 eV. Thus, isomer **10A** is assigned as the most probable structure for VGe_{10}^- detected in our experiments, but the existence of **10B** cannot be ruled out.

VGe_{11}^-. The most stable structure of VGe_{11}^- (isomer **11A**) can be generated by addition of three Ge atoms on the top of the boat-shaped structure of VGe_8^- (**8A**) with two Ge atoms interacting with two ends of the boat, respectively, and the third Ge atom bridging the two Ge atoms. Isomer **11B** can be formed by capping a Ge atom on the VGe_{10} oblique pentagonal prism. Isomer **11C** can be described as a basket-shaped structure with two Ge atoms forming the handle of the basket, the other Ge atoms forming the containing part of the basket, and the V atom encapsulated into the basket. Isomers **11B** and **11C** are higher in energy than **11A** by 0.13 and 0.60 eV, respectively. The calculated VDE of **11A** (3.71 eV) is in good agreement with the experimental value (3.85 eV), while those of **11B** (3.52 eV) and **11C** (3.23 eV) are much lower than the experimental value. Thus, isomer **11A** is regarded as the most probable one observed in our experiments.

VGe_{12}^-. We found that the most stable isomer of VGe_{12}^- (**12A**) is a D_{3d} distorted hexagonal prism structure with the V atom at the center. It can also be viewed as a double-chair style hexagonal cage structure. Its VDE is calculated to be 3.63 eV, which is in agreement with the experimental measurement (3.7 eV). Isomers **12B** and **12C** are higher than **12A** by 0.37 and 0.45 eV, respectively, much less stable than isomer **12A**. Therefore, their existence in the experiments can be ruled out. We suggest isomer **12A** to be the most probable structure detected in our experiments. Isomer **12A** is similar to the structure of $CuSi_{12}^-$ reported previously.[49] The theoretical calculations of Tang et al. suggested the most stable structure of neutral VGe_{12} cluster to be a pseudoicosahedron.[22] In this work, we have considered many initial structures for VGe_{12}^- cluster, including those reported in the literature. We found that the pseudoicosahedron type of structure is less stable. Huang et al. found that VSi_{12}^- has a D_{6h} hexagonal prism cage structure.[50] Here, we found the structure of VGe_{12}^- is slightly distorted to lower symmetry compared to the D_{6h} structure of VSi_{12}^-, more likely because the Ge atom has larger radius than the Si atom.

4.2. Neutral VGe_n (n = 3−12) Clusters. We have also investigated the structures of the neutral VGe_n (n = 3−12) clusters with DFT calculations at B3PW91/6-311+G(d) level and displayed them in Figure 3. The most stable structures of the neutral VGe_n clusters are almost identical to those of VGe_n^-,

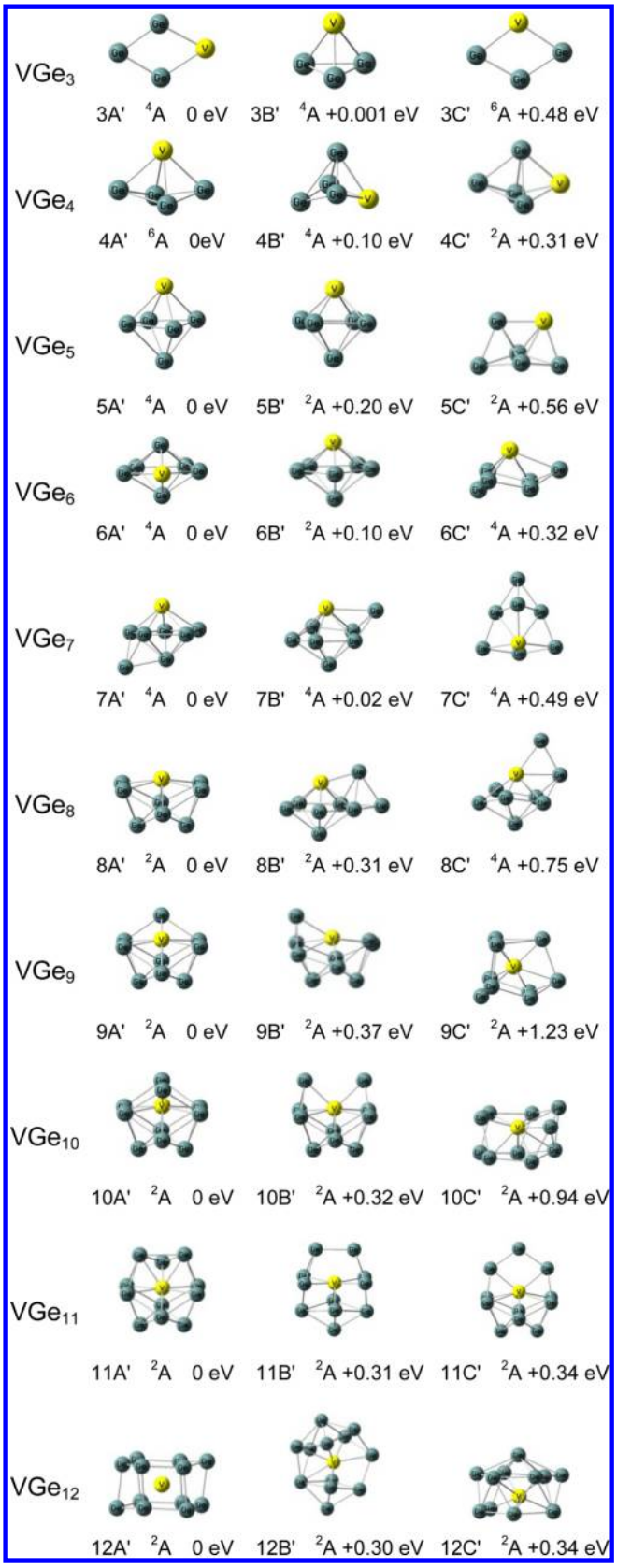

Figure 3. Geometries of the typical low-lying isomers of VGe_n (n = 3−12) clusters. The relative energies to the most stable isomers are shown.

DOI: 10.1021/jp511694c
J. Phys. Chem. C 2015, 119, 11048−11055

except that the structures of VGe_6, VGe_7, and VGe_{11} are slightly different from their corresponding anions. For VGe_6, the most stable isomer (**6A′**) is a pentagonal bipyramid with the V atom at the equatorial ring, which is similar to isomer **6C** of VGe_6^-. The second isomer (**6B′**) is similar to the most stable structure of VGe_6^- anion (**6A**, pentagonal bipyramid with the V atom at the vertex), and it is higher than **6A′** by 0.10 eV. As for VGe_7, isomers **7A′** and **7B′** can be seen as a Ge atom capping on different faces of VGe_6 pentagonal bipyramid, and they are nearly degenerate in energy with **7B′** being higher than **7A′** by only 0.02 eV. The structure of **7B′** is close to the most stable structure of VGe_7^- (**7A**). The most stable isomer of VGe_{11} (**11A′**) can be viewed as a Ge_3 triangle capping on the boat-shaped structure of VGe_8. Therefore, the cage structure of the neutral VGe_{11} is closed more tightly than that of the anion.

5. DISCUSSION

The dominant structures of the small size anionic and neutral VGe_n clusters, with n = 3−7, are exdohedral structures, which adopt the geometries of Ge_n or Ge_{n+1}, with the V atom at adsorption or substitutional sites.[51−53] At n = 8, the $VGe_n^{-/0}$ clusters show half-endohedral boat-shaped structures, and the opening of the boat-shaped structure is gradually covered by the additional Ge atoms to form Ge_n cage from n = 9 to 11. At n = 12, a D_{3d} distorted hexagonal prism cage structure is formed. The structures of $VGe_{12}^{-/0}$ are not simply evolved from the boat-shaped structures of $VGe_8^{-/0}$ due to the formation of more symmetric geometries. The water adsorption reactivity experiment conducted by Atobe et al. showed that the water adsorption reactivity of VGe_n^+ decreased quickly at n = 8, and there is almost no reactivity at VGe_{12}^+.[34] The structural evolution of VGe_n clusters found in this work is consistent with the water adsorption reactivity experiment of VGe_n^+ clusters. It seems that the changes of VGe_n^- photoelectron spectra are related to their structural evolution. The VDE of VGe_4^- is higher than that of VGe_3^- by 0.45 eV, probably due to the 2D to 3D structure transition. The spectral profiles of VGe_5^-, VGe_6^-, and VGe_7^- are rather similar except that their VDEs increase gradually with the number of Ge atoms. That is more likely related to their similar structures. In addition, the significant increase of VDE and change of spectral profile at n = 8 may be associated with the formation of half-endohedral boat-shaped structure. The structures of VGe_9^- and VGe_{10}^- are derived from the boat-shaped structure of VGe_8^-, which perhaps gives them similar spectral profiles.

It is also interesting to compare the structures of VGe_n^- with those of VSi_n^-. The structures of VSi_n^- (n = 3−6) have been reported by Xu et al.[31] and that of VSi_{12}^- by Huang et al.[50] There is no report of the structures of VSi_{7-11}^- in the literature. Thus, we conducted DFT calculations on the VSi_{7-11}^- clusters and presented them in the Supporting Information (Table S2 and Figure S1). We found that the structural evolution of VGe_n^- is very similar to that of VSi_n^-, except that the most stable structures of VGe_3^-, VGe_{10}^-, and VGe_{12}^- are slightly different from those of VSi_3^-, VSi_{10}^-, and VSi_{12}^-. The most stable structure of VGe_3^- is a rhombus instead of a tetrahedron in the case of VSi_3^-. The most stable structure of VGe_{10}^- is similar to the second stable isomer of VSi_{10}^-. The structure of VGe_{12}^- is slightly distorted to lower symmetry compared to the D_{6h} structure of VSi_{12}^-. The clusters with n = 8 show half-encapsulated boat-shaped structures, and the opening of the boat-shaped structure is gradually covered by the additional Ge or Si atoms. The H_2O adsorption reactivity experiments of VSi_n^- conducted by Koyasu et al.[54] showed that the adsorption reactivity of VSi_n^- decreases dramatically starting at n = 8 and reaches a minima at n = 9−12. These phenomenons are consistent with the encapsulation of the V atom into the Si or Ge cages.

Here, we investigate the electronic and magnetic properties of the VGe_n (n = 3−12) clusters. The natural population analyses (NPA) were conducted for the most stable isomers of the anionic and neutral VGe_n (n = 3−12) clusters. The results are shown in Table 3. It is found that the negative charge is mainly localized on the Ge atoms for the small size, with n = 3−6, then there is slight electron transfer from the Ge_n framework to the V atom at n = 7. For cluster size of n = 8−12, the negative charge on the V atom increases significantly, suggesting that there is more electron transfer from the Ge_n framework to the V atom. The transfer of electron from the Ge atoms to the V atom is related to the formation of endohedral structures. We also found that the magnetic moments of the VGe_n clusters decrease dramatically upon the formation of endohedral cage structures. For the cluster size of n = 3−7, the total magnetic moments of VGe_n^- anion are 4 or 2 μ_B, and those of the neutral VGe_n are 3 or 5 μ_B. For n = 8−12, the total magnetic moments of the anionic clusters decrease to 0 and those of the neutral clusters decrease to 1 μ_B. These results are similar to those of $CoGe_n^{-/0}$ (n = 2−11) clusters.[55]

Table 3. NPA Charges, Atomic Magnetic Moments (μ_A), Total Magnetic Moments (μ_T) of the Most Stable Isomers of Anionic and Neutral VGe_n (n = 3−12) Clusters

cluster	NPA charge on V (e)	μ_T (μ_B)	μ_V (μ_B)
VGe_3^-	0.01	4	4.17
VGe_4^-	−0.06	2	3.11
VGe_5^-	−0.33	2	3.10
VGe_6^-	−0.41	2	3.05
VGe_7^-	−0.75	2	2.81
VGe_8^-	−1.85	0	0
VGe_9^-	−2.80	0	0
VGe_{10}^-	−4.92	0	0
VGe_{11}^-	−3.32	0	0
VGe_{12}^-	−3.25	0	0
VGe_3	0.58	3	3.44
VGe_4	0.29	5	4.07
VGe_5	0.27	3	3.37
VGe_6	0.28	3	3.40
VGe_7	−0.12	3	3.27
VGe_8	−1.55	1	0.83
VGe_9	−2.64	1	1.03
VGe_{10}	−4.11	1	0.89
VGe_{11}	−4.80	1	1.04
VGe_{12}	−3.38	1	0.37

To further investigate the bonding properties of the VGe_{12}^- cluster, the molecular orbitals of the most stable isomer of VGe_{12}^- (**12A**) were analyzed and displayed in Figure 4. The HOMO of VGe_{12}^- is mainly composed by the $3d_{x^2-y^2}$ orbital of the V atom and the 4*s*4*p* hybridized orbitals of the Ge atoms, while the HOMO−1 of VGe_{12}^- involves the $3d_{xy}$ orbital of the V atom and the 4*s*4*p* hybridized orbitals of the Ge atoms. The HOMO−2 has an interesting sandwich shape with the electron cloud delocalized in the planes of the pair of six-membered Ge rings, more likely due to the interactions between the V $4p_z$ orbital and the Ge 4*s*4*p* hybridized orbitals. The HOMO−3 has the components from the V $3d_{xz}$ and Ge 4*s*4*p* orbitals. These molecular orbitals illustrate that there are strong interactions between the V and Ge atoms. The valent electrons of the V and

DOI: 10.1021/jp511694c
J. Phys. Chem. C 2015, 119, 11048−11055

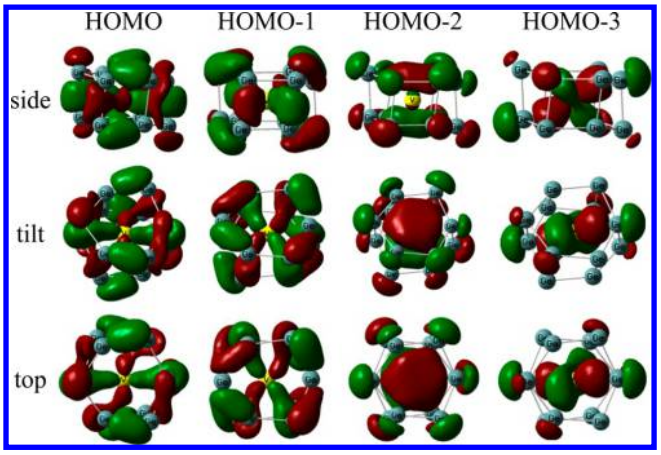

Figure 4. Molecular orbitals of VGe_{12}^- cluster viewed from different angles.

Ge atoms are delocalized over the whole VGe_{12}^- cluster with most of them surrounding the V atom. It seems that the strong delocalized V−Ge ligand interactions strengthen the V−Ge bonds, therefore, make the D_{3d} distorted hexagonal prism structure of VGe_{12}^- stable.

6. CONCLUSIONS

We investigated the structural, electronic and magnetic properties of $VGe_n^{-/0}$ (n = 3−12) clusters using anion photoelectron spectroscopy and DFT calculations. For both anionic and neutral VGe_n clusters, with $n \leq 7$, the dominant geometries are exohedral structures. At n = 8, the $VGe_n^{-/0}$ clusters show half-endohedral boat-shaped structures, and the opening of the boat-shaped structure is gradually covered by the additional Ge atoms to form Ge_n cage from n = 9 to 11. At n = 12, a D_{3d} distorted hexagonal prism cage structure is formed. At n = 8−12, the electron transfer from the Ge_n framework to the V atom and the magnetic moments also decrease to the lowest values. The charge transfer pattern and the minimization of the magnetic moments are related to the structural evolution.

■ ASSOCIATED CONTENT

Supporting Information

The Cartesian coordinates of low-lying isomers of VGe_n^- (n = 3−12), and the theoretical results of VSi_n^- (n = 7−11) clusters are listed. This material is available free of charge via the Internet at http://pubs.acs.org.

■ AUTHOR INFORMATION

Corresponding Authors

*E-mail: xuhong@iccas.ac.cn.

*E-mail: zhengwj@iccas.ac.cn. Tel.: +86 10 62635054. Fax: +86 10 62563167.

Notes

The authors declare no competing financial interest.

■ ACKNOWLEDGMENTS

This work was supported by the Knowledge Innovation Program of the Chinese Academy of Sciences (Grant No. KJCX2-EW-H01) and the Natural Science Foundation of China (Grant No. 21103202). The theoretical calculations were conducted on the ScGrid and DeepComp 7000 of the Supercomputing Center, Computer Network Information Center of the Chinese Academy of Sciences.

■ REFERENCES

(1) Kamata, Y. High-K/Ge Mosfets for Future Nanoelectronics. *Mater. Today* **2008**, *11*, 30−38.

(2) Pillarisetty, R. Academic and Industry Research Progress in Germanium Nanodevices. *Nature* **2011**, *479*, 324−328.

(3) Zhang, X.; Li, G. L.; Gao, Z. Laser Ablation of Co/Ge Mixtures: A New Type of Endohedral Structure, a Semiconductor Cage Trapping a Metal Atom. *Rapid Commun. Mass Spectrom.* **2001**, *15*, 1573−1576.

(4) Furuse, S.; Koyasu, K.; Atobe, J.; Nakajima, A. Experimental and Theoretical Characterization of MSi_{16}^-, MGe_{16}^-, MSn_{16}^-, and MPb_{16}^- (M = Ti, Zr, and Hf): The Role of Cage Aromaticity. *J. Chem. Phys.* **2008**, *129*, 064311.

(5) Wang, J.; Han, J. G. A Theoretical Study on Growth Patterns of Ni-Doped Germanium Clusters. *J. Phys. Chem. B* **2006**, *110*, 7820−7827.

(6) Zhao, W.-J.; Wang, Y.-X. Geometries, Stabilities, and Electronic Properties of $FeGe_n$ (n = 9−16) Clusters: Density-Functional Theory Investigations. *Chem. Phys.* **2008**, *352*, 291−296.

(7) Li, G. L.; Zhang, X.; Tang, Z. C.; Gao, Z. Theoretical Studies on the Structure of the Endohedral $CoGe_{10}^-$ Cluster Anion. *Chem. Phys. Lett.* **2002**, *359*, 203−212.

(8) Wang, J.; Han, J. G. A Computational Investigation of Copper-Doped Germanium and Germanium Clusters by the Density-Functional Theory. *J. Chem. Phys.* **2005**, *123*, 244303.

(9) Hou, X. J.; Gopakumar, G.; Lievens, P.; Nguyen, M. T. Chromium-Doped Germanium Clusters $CrGe_n$ (n = 1−5): Geometry, Electronic Structure, and Topology of Chemical Bonding. *J. Phys. Chem. A* **2007**, *111*, 13544−13553.

(10) Wang, J.; Han, J.-G. The Growth Behaviors of the Zn-Doped Different Sized Germanium Clusters: A Density Functional Investigation. *Chem. Phys.* **2007**, *342*, 253−259.

(11) Li, X. J.; Su, K. H. Structure, Stability and Electronic Property of the Gold-Doped Germanium Clusters: $AuGe_n$ (n = 2−13). *Theor. Chem. Acc.* **2009**, *124*, 345−354.

(12) Zhao, W.-J.; Wang, Y.-X. Geometries, Stabilities, and Magnetic Properties of $MnGe_n$ (n = 2−16) Clusters: Density-Functional Theory Investigations. *J. Mol. Struct.: THEOCHEM* **2009**, *901*, 18−23.

(13) Kapila, N.; Jindal, V. K.; Sharma, H. Structural, Electronic, and Magnetic Properties of Mn, Co, Ni in Ge_n for (n = 1−13). *Phys. B: Condens. Matter* **2011**, *406*, 4612−4619.

(14) Tai, T. B.; Nguyen, M. T. Enhanced Stability by Three-Dimensional Aromaticity of Endohedrally Doped Clusters $X_{10}M^{0/-}$ with X = Ge, Sn, Pb and M = Cu, Ag, Au. *J. Phys. Chem. A* **2011**, *115*, 9993−9999.

(15) Uta, M. M.; Cioloboc, D.; King, R. B. Cobalt-Centered Ten-Vertex Germanium Clusters: The Pentagonal Prism as an Alternative to Polyhedra Predicted by the Wade-Mingos Rules. *Inorg. Chem.* **2012**, *51*, 3498−3504.

(16) Li, X. J.; Su, K. H.; Yang, X. H.; Song, L. M.; Yang, L. M. Size-Selective Effects in the Geometry and Electronic Property of Bimetallic Au-Ge Nanoclusters. *Comput. Theor. Chem.* **2013**, *1010*, 32−37.

(17) Kumar, V.; Singh, A. K.; Kawazoe, Y. Smallest Magic Caged Clusters of Si, Ge, Sn, and Pb by Encapsulation of Transition Metal Atom. *Nano Lett.* **2004**, *4*, 677−681.

(18) Wang, J.; Han, J. G. Geometries and Electronic Properties of the Tungsten-Doped Germanium Clusters: WGe_n (n = 1−17). *J. Phys. Chem. A* **2006**, *110*, 12670−12677.

(19) Jing, Q.; Tian, F. Y.; Wang, Y. X. No Quenching of Magnetic Moment for the Ge_nCo (n = 1−13) Clusters: First-Principles Calculations. *J. Chem. Phys.* **2008**, *128*, 124319.

(20) Bandyopadhyay, D.; Kaur, P.; Sen, P. New Insights into Applicability of Electron-Counting Rules in Transition Metal Encapsulating Ge Cage Clusters. *J. Phys. Chem. A* **2010**, *114*, 12986−12991.

(21) Bandyopadhyay, D.; Sen, P. Density Functional Investigation of Structure and Stability of Ge_n and Ge_nNi (n = 1−20) Clusters: Validity of the Electron Counting Rule. *J. Phys. Chem. A* **2010**, *114*, 1835−1842.

(22) Tang, C. M.; Liu, M. Y.; Zhu, W. H.; Deng, K. M. Probing the Geometric, Optical, and Magnetic Properties of 3d Transition-Metal

DOI: 10.1021/jp511694c
J. Phys. Chem. C 2015, 119, 11048−11055

Endohedral $Ge_{12}M$ (M = Sc-Ni) Clusters. *Comput. Theor. Chem.* **2011**, *969*, 56−60.
(23) Bandyopadhyay, D. Architectures, Electronic Structures, and Stabilities of Cu Doped Ge_n Clusters: Density Functional Modeling. *J. Mol. Model.* **2012**, *18*, 3887−3902.
(24) Kumar, M.; Bhattacharyya, N.; Bandyopadhyay, D. Architecture, Electronic Structure and Stability of $TM@Ge_n$ (TM = Ti, Zr, and Hf; n = 1−20) Clusters: A Density Functional Modeling. *J. Mol. Model.* **2012**, *18*, 405−418.
(25) Dhaka, K.; Trivedi, R.; Bandyopadhyay, D. Electronic Structure and Stabilities of Ni-Doped Germanium Nanoclusters: A Density Functional Modeling Study. *J. Mol. Model.* **2013**, *19*, 1473−1488.
(26) Kumar, V.; Kawazoe, Y. Metal-Encapsulated Caged Clusters of Germanium with Large Gaps and Different Growth Behavior Than Silicon. *Phys. Rev. Lett.* **2002**, *88*, 235504.
(27) Lu, J.; Nagase, S. Metal-Doped Germanium Clusters MGe_n at the Sizes of n = 12 and 10: Divergence of Growth Patterns from the MSi_n Clusters. *Chem. Phys. Lett.* **2003**, *372*, 394−398.
(28) Neukermans, S.; Wang, X.; Veldeman, N.; Janssens, E.; Silverans, R. E.; Lievens, P. Mass Spectrometric Stability Study of Binary MS_n Clusters (S = Si, Ge, Sn, Pb, and M = Cr, Mn, Cu, Zn). *Int. J. Mass Spectrom.* **2006**, *252*, 145−150.
(29) Wang, J.; Han, J. G. A Computational Investigation of Copper-Doped Germanium and Germanium Clusters by the Density-Functional Theory. *J. Chem. Phys.* **2005**, *123*, 244303.
(30) Wang, J.; Han, J. G. The Growth Behaviors of the Zn-Doped Different Sized Germanium Clusters: A Density Functional Investigation. *Chem. Phys.* **2007**, *342*, 253−259.
(31) Xu, H. G.; Zhang, Z. G.; Feng, Y.; Yuan, J.; Zhao, Y.; Zheng, W. Vanadium-Doped Small Silicon Clusters: Photoelectron Spectroscopy and Density-Functional Calculations. *Chem. Phys. Lett.* **2010**, *487*, 204−208.
(32) Xu, H.-G.; Kong, X.-Y.; Deng, X.-J.; Zhang, Z.-G.; Zheng, W.-J. Smallest Fullerene-Like Silicon Cage Stabilized by a V_2 Unit. *J. Chem. Phys.* **2014**, *140*, 024308.
(33) Singh, A. K.; Kumar, V.; Kawazoe, Y. Metal Encapsulated Nanotubes of Germanium with Metal Dependent Electronic Properties. *Eur. Phys. J. D* **2005**, *34*, 295−298.
(34) Atobe, J.; Koyasu, K.; Furuse, S.; Nakajima, A. Anion Photoelectron Spectroscopy of Germanium and Ti_n Clusters Containing a Transition-or Lanthanide-Metal Atom; MGe_n^- (n = 8−20) and MSn_n^- (n = 15−17) (M = Sc-V, Y-Nb, and Lu-Ta). *Phys. Chem. Chem. Phys.* **2012**, *14*, 9403−9410.
(35) Frisch, M. J.; Trucks, G. W.; Schlegel, H. B.; Scuseria, G. E.; Robb, M. A.; Cheeseman, J. R.; Scalmani, G.; Barone, V.; Mennucci, B.; Petersson, G. A.; et al. *Gaussian 09*, Revision A.02; Gaussian, Inc.: Wallingford, CT, 2009.
(36) Becke, A. D. Density-Functional Thermochemistry 3. The Role of Exact Exchange. *J. Chem. Phys.* **1993**, *98*, 5648−5652.
(37) Perdew, J. P.; Chevary, J. A.; Vosko, S. H.; Jackson, K. A.; Pederson, M. R.; Singh, D. J.; Fiolhais, C. Atoms, Molecules, Solids, and Surfaces: Applications of the Generalized Gradient Approximation for Exchange and Correlation. *Phys. Rev. B* **1992**, *46*, 6671−6687.
(38) Perdew, J. P.; Chevary, J. A.; Vosko, S. H.; Jackson, K. A.; Pederson, M. R.; Singh, D. J.; Fiolhais, C. Atoms, Molecules, Solids, and Surfaces: Applications of the Generalized Gradient Approximation for Exchange and Correlation. *Phys. Rev. B* **1993**, *48*, 4978−4978.
(39) Perdew, J. P.; Burke, K.; Wang, Y. Generalized Gradient Approximation for the Exchange-Correlation Hole of a Many-Electron System. *Phys. Rev. B* **1996**, *54*, 16533−16539.
(40) Kumar, M.; Bhattacharyya, N.; Bandyopadhyay, D. Architecture, Electronic Structure and Stability of $TM@Ge_n$ (TM = Ti, Zr, and Hf; n = 1−20) Clusters: A Density Functional Modeling. *J. Mol. Model.* **2012**, *18*, 405−418.
(41) Foster, J. P.; Weinhold, F. Natural Hybrid Orbitals. *J. Am. Chem. Soc.* **1980**, *102*, 7211−7218.
(42) Reed, A. E.; Weinhold, F. Natural Bond Orbital Analysis of near-Hartree-Fock Water Dimer. *J. Chem. Phys.* **1983**, *78*, 4066−4073.
(43) Reed, A. E.; Weinhold, F. Natural Localized Molecular-Orbitals. *J. Chem. Phys.* **1985**, *83*, 1736−1740.
(44) Reed, A. E.; Weinstock, R. B.; Weinhold, F. Natural-Population Analysis. *J. Chem. Phys.* **1985**, *83*, 735−746.
(45) Carpenter, J. E. Extension of Lewis structure concepts to open-shell and excited-state molecular species, Ph. D. thesis, University of Wisconsin, Madison, WI, 1987.
(46) Reed, A. E.; Curtiss, L. A.; Weinhold, F. Intermolecular Interactions from a Natural Bond Orbital, Donor-Acceptor Viewpoint. *Chem. Rev.* **1988**, *88*, 899−926.
(47) Weinhold, F.; Carpenter, J. E. In *The Structure of Small Molecules and Ions*; Naaman, R., Vager, Z., Eds.; Plenum: New York, 1988; p 227.
(48) Carpenter, J. E.; Weinhold, F. Analysis of The Geometry of The Hydroxymethyl Radical by The "Different Hybrids for Different Spins" Natural Bond Orbital Procedure. *J. Mol. Struct.: THEOCHEM* **1988**, *169*, 41−62.
(49) Xu, H. G.; Wu, M. M.; Zhang, Z. G.; Yuan, J. Y.; Sun, Q.; Zheng, W. J. Photoelectron Spectroscopy and Density Functional Calculations of $CuSi_n^-$ (n = 4−18) Clusters. *J. Chem. Phys.* **2012**, *136*, 104308.
(50) Huang, X.; Xu, H.-G.; Lu, S.; Su, Y.; King, R. B.; Zhao, J.; Zheng, W. Discovery of a Silicon-Based Ferrimagnetic Wheel Structure in $V_xSi_{12}^-$ (x = 1−3) Clusters: Photoelectron Spectroscopy and Density Functional Theory Investigation. *Nanoscale* **2014**, *6*, 14617−14621.
(51) Lanza, G.; Millefiori, S.; Millefiori, A.; Dupuis, M. Geometries and Energies of Small Ge_n (n = 2−6) Clusters: An Ab Initio Molecular-Orbital Study. *J. Chem. Soc., Faraday Trans.* **1993**, *89*, 2961−2967.
(52) Li, B. X.; Cao, P. L.; Song, B.; Ye, Z. Z. Electronic and Geometric Structures of Ge_n^- and Ge_n^+ (n = 5−10) Clusters in Comparison with Corresponding Si_n Ions. *Phys. Lett. A* **2003**, *307*, 318−325.
(53) Xu, W. G.; Zhao, Y.; Li, Q. S.; Xie, Y. M.; Schaefer, H. F. The Germanium Clusters Ge_n^- (n = 1−6) and Their Anions: Structures, Thermochemistry and Electron Affinities. *Mol. Phys.* **2004**, *102*, 579−598.
(54) Koyasu, K.; Atobe, J.; Akutsu, M.; Mitsui, M.; Nakajima, A. Electronic and Geometric Stabilities of Clusters with Transition Metal Encapsulated by Silicon. *J. Phys. Chem. A* **2007**, *111*, 42−49.
(55) Deng, X. J.; Kong, X. Y.; Xu, X. L.; Xu, H. G.; Zheng, W. J. Structural and Magnetic Properties of $CoGe_n^-$ (n = 2−11) Clusters: Photoelectron Spectroscopy and Density Functional Calculations. *ChemPhysChem* **2014**, *15*, 3987−3993.

DOI: 10.1021/jp511694c
J. Phys. Chem. C 2015, 119, 11048−11055